Inkjet Printing of Bioadhesives

Anand Doraiswamy,[1] Timothy M. Dunaway,[2] Jonathan J. Wilker,[2] Roger J. Narayan[1]

[1] Joint Department of Biomedical Engineering, University of North Carolina at Chapel Hill, Chapel Hill, North Carolina 27599-7575

[2] Department of Chemistry, Purdue University, West Lafayette, Indiana 47907-2084

Received 6 February 2008; revised 24 April 2008; accepted 3 June 2008
Published online 19 August 2008 in Wiley InterScience (www.interscience.wiley.com). DOI: 10.1002/jbm.b.31183

Abstract: Over the past century, synthetic adhesives have largely displaced their natural counterparts in medical applications. However, rising concerns over the environmental and toxicological effects of the solvents, monomers, and additives used in synthetic adhesives have recently led the scientific community to seek natural substitutes. Marine mussel adhesive protein is a formaldehyde-free natural adhesive that demonstrates excellent adhesion to several classes of materials, including glasses, metals, metal oxides, and polymers. In this study, we have demonstrated computer aided design (CAD) patterning of various biological adhesives using piezoelectric inkjet technology. A MEMS-based piezoelectric actuator was used to control the flow of the mussel adhesive protein solution through the ink jet nozzles. Fourier transform infrared spectroscopy (FTIR), microscopy, and adhesion studies were performed to examine the chemical, structural, and functional properties of these patterns, respectively. FTIR revealed the piezoelectric inkjet technology technique to be nondestructive. Atomic force microscopy was used to determine the extent of chelation caused by Fe(III). The adhesive strength in these materials was correlated with the extent of chelation by Fe(III). Piezoelectric inkjet printing of naturally-derived biological adhesives may overcome several problems associated with conventional tissue bonding materials. This technique may significantly improve wound repair in next generation eye repair, fracture fixation, wound closure, and drug delivery devices. © 2008 Wiley Periodicals, Inc. J Biomed Mater Res Part B: Appl Biomater 89B: 28–35, 2009

Keywords: biomaterials; thin film; bioadhesive; microfabrication

INTRODUCTION

Suturing is the "gold standard" joining technique for many medical procedures. Unfortunately, the use of suture materials requires long operating times as well as significant surgical skill. In addition, use of sutures is associated with several complications, including granulomas, postoperative epithelial ingrowth, postoperative discomfort, infection, and inflammation. Furthermore, sutures may place excess tension on tissues, leading to tissue warping. An alternative joining technique that has gained support over the past few years involves the use of adhesives, which hold tissue together for several weeks while inflammatory and tissue regrowth processes allow the defect to heal. Medical adhesives must perform several functions, which include degrading in order to allow complete healing at the lesion site and providing sufficient tensile strength for the intended application.

Conventional adhesives and techniques suffer from biocompatibility and safety issues. For example, tissue sealants derived from cyanoacrylate esters (Dermabond®, Indermil®, Nexaband®, and Vetbond®) are used in repairing tendon, tooth enamel, cornea, and skin tissues.[1–5] Unfortunately, cyanoacrylate adhesives are nonbiodegradable and permanently remain at the treatment site. As a result, these materials have the potential to induce local inflammation, neovascularization, foreign body reaction, and necrosis.[6–8] In addition, these materials can demonstrate dose-dependent carcinogenic and toxic properties. Fibrin sealants (derived from human blood coagulation factors) have also been considered for use in a variety of surgical and endoscopic applications.[9–11] For example, Beriplast® P is a fibrin sealant that contains Combiset-1 [aprotinin (bovine), factor XIII (human), and fibrinogen (human)] and Combiset-2 (calcium chloride and thrombin (human)); these components are mixed in the operating room. The components obtained from pooled human plasma (fibrinogen, factor XIII, and thrombin) undergo various sterilization, manufac-

Correspondence to: Prof. R. J. Narayan (e-mail: roger_narayan@unc.edu)
Contract grant sponsors: National Science Foundation; National Institutes of Health; Office of Naval Research

turing, and pasteurization measures. However, there are several safety issues that have limited the use of these materials, including the possibility of disease transmission. For example, the risk of HIV in blood-derived materials screened with the p24 HIV-1 antigen test is currently estimated at 1:700,000.[12] Concerns also exist regarding the transmission of human T-cell lymphotropic virus-1, hepatitis A virus, hepatitis B virus, hepatitis C virus, Parvovirus B19, and spongiform encephalopathy agents from blood-derived materials. Surgeons and their patients require improved tissue joining materials and methods.

Mussel adhesive proteins are natural adhesives secreted by sedentary mollusks (mussels) that inhibit intertidal and subtidal areas. An attachment plaque known as a byssus allows mussels to form strong attachments to underwater surfaces. *Mytilus edulis* (common blue mussel) is one of the most widely studied mussels.[14–23] It produces several unique adhesive proteins, including *Mytilus edulis* foot protein-1 (Mefp-1), *Mytilus edulis* foot protein-2 (Mefp-2), *Mytilus edulis* foot protein-3 (Mefp-3), *Mytilus edulis* foot protein-4 (Mefp-4), and *Mytilus edulis* foot protein-5 (Mefp-5). These proteins contain up to 30 mole percent 3,4-dihydroxyphenyl-L-alanine (DOPA), which is a molecule created by hydroxylation of the aromatic ring in the amino acid tyrosine. It has been suggested that DOPA drives the adhesion of a mussel plaque to an environmental surface by means of hydrogen bonding, metal-mediated catechol complexation, and/or weak physical interactions.[14–23]

Rapid prototyping is a technology originally developed approximately thirty years ago for the preparation of machine tool prototypes. One possible application for rapid prototyping technology is microscale processing of biomaterials. Computer aided design (CAD) rapid prototyping techniques such as inkjet printing may allow for high throughput patterning of biological materials for medical applications.[24–26] In piezoelectric inkjet printers, the print head consist of a piezoelectric transducer, nozzle, manifold, pumping chamber, and inlet passage. Piezoelectric printers are categorized based on the deformation mode of the lead zirconate titanate piezoelectric crystal (e.g., squeeze, bend, push or shear). When a voltage is applied to the lead zirconate titanate piezoelectric transducer, the transducer deforms. Mechanical vibrations and acoustic waves are generated. When a given linear velocity is reached by the fluid, it is ejected from the orifice as a droplet. Ink jet printers can dispense fluid droplets with volumes in the picoliter to microliter range. The resolution of patterns fabricated using piezoelectric ink jet printing is determined by several factors, including ink viscosity, ink surface tension, ink droplet size, and printerhead resolution. Unlike thermal inkjet printers, the ink used in piezoelectric inkjet printers does not undergo heating and cooling cycles. We have recently demonstrated that piezoelectric inkjet deposition is a powerful, noncontact, and nondestructive technique for patterning many biological materials, including streptavidin protein, monofunctional acrylate esters, sinapinic acid, deoxyribonucleic acid, and multiwalled carbon nanotube/DNA hybrid materials.[27]

In this study, we have demonstrated CAD patterning of various biological adhesives using piezoelectric inkjet technology. Fourier transform infrared spectroscopy (FTIR), atomic force microscopy, and adhesion studies were performed to examine the chemical, structural, and functional properties of these patterns, respectively. This technique may significantly improve wound repair in next generation eye repair, fracture fixation, wound closure, and drug delivery devices.

MATERIALS AND METHODS

Mussel adhesive proteins (Mefp-1 and Mefp-2) were extracted from marine mussel feet as described in[28] with slight modification. The protein pellets were extracted with water, rather than the reported acetic acid.[28] The extract yields a solution that contains predominantly two proteins, ~80% Mefp-1 and ~20% Mefp-2.[28] The final DOPA concentration in this solution was 0.16 mM, the total protein concentration in this solution was ~2 μM, and the viscosity of this solution was similar to water (density ~1 g/mL). To study iron-induced cross-linking, a $FeCl_3$ solution was prepared in series dilution to obtain ratios of 1:1 Fe:DOPA, 10:1 Fe:DOPA, and 100:1 Fe:DOPA. *N*-Butyl cyanoacrylate (Vetbond® Tissue Adhesive) was obtained from a commercial source (3M, St. Paul, MN). 2-Octyl cyanoacrylate (Nexaband® Liquid Topical Tissue Adhesive) was obtained from a commercial source (Abbott Laboratories, North Chicago, IL). Ethyl cyanoacrylate (Loctite® Quick Set Adhesive) was obtained from a commercial source (Ted Pella, Redding, CA).

The DMP 2800 piezoelectric inkjet printer (FujiFilm Dimatix, Santa Clara, CA) is based on a cartridge printhead system. Fluid was injected into the fluid module. The fluid module was then attached to the jetting module to form a sealed cartridge. The inkjet print head itself consists of a silicon die with sixteen individually addressable jets, which are spaced 254 μm apart. The effective nozzle diameter is 21.5 μm, which provides droplets that are ~10 pL in volume. The waveform pulse shape (amplitude, slew rate, and duration), frequency and voltage were optimized for each adhesive solution independently. The droplet flight (distance traveled) from the nozzle was recorded using an ultra-fast camera. The protein solution was also inkjetted at several voltage values (10, 20, 30, and 40 V) in order to study the effect of voltage on protein structure. The images were recorded at 30 μs intervals at several voltage values.

Approximately 10 μL of the adhesives were inkjetted at a temperature of 25°C and at 40% relative humidity into uniform 1 cm^2 patterns; dispensed volume was determined using the DMP2800 software based on pattern and drop parameters. Adhesives were deposited on Si(111) substrates for optical, AFM, XPS, and contact angle measurements; on full-thickness porcine skin substrates for adhesion test-

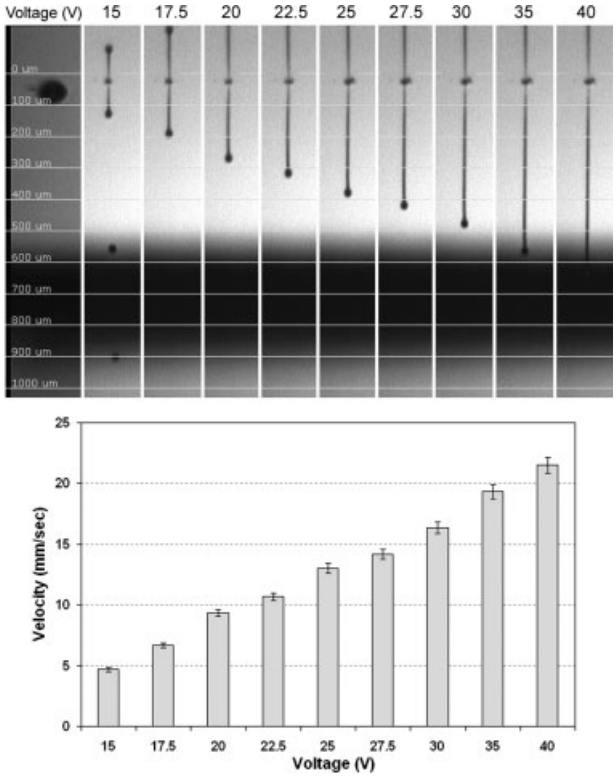

Figure 1. Optical micrograph of mussel adhesive protein solution inkjetted at several voltages (15–40 V) and captured at 30 μs time delay. A corresponding plot of mean velocity of inkjetted solution plotted versus firing voltage is also shown. Bar indicates standard deviation of mean velocity ($p < 0.05$).

ing; and on KCl and AgCl substrates for FTIR measurements. To examine iron-induced cross-linking, mussel adhesive protein solution was inkjetted. A layer of $FeCl_3$ solution (at varying concentrations to reach 1:1, 10:1, 100:1 Fe: DOPA, respectively) was subsequently inkjetted using the identical pattern. Dropcast samples were prepared for the FITR studies.

Fourier transform infrared (FTIR) was performed using a Mattson 5000s spectrometer with 4 cm^{-1} resolution, which was operated in transmission mode. Atomic force microscopy (AFM) was performed using a *N*-scriptor system (Nanoink, Chicago, IL). Three-dimensional analysis was performed using SPM Nanorule® software (Nanoink, Chicago, IL). X-ray photoelectron spectra was acquired using an LAS-3000 spectrometer (Riber, Rueil-Malmaison, France) with a Mg Kα source ($\lambda = 1254$ eV) and a 1 mm spot size. The take off angle was 75° from the surface, the X-ray incidence angle was 20°, and the X-ray source-analyzer angle was 55°. The base pressure in the analysis chamber was $\sim 10^{-10}$ Torr. Contact-angle studies were performed using a goniometer consisting of a syringe, an aligned digital zoom camera, and an illumination source. Adhesion studies were performed with butt joints on full-thickness porcine skin substrates using an 8501 uniaxial tensile test system (Instron, Norwood, MA), which has a load range of load range ± 10 kN. The adhesion testing

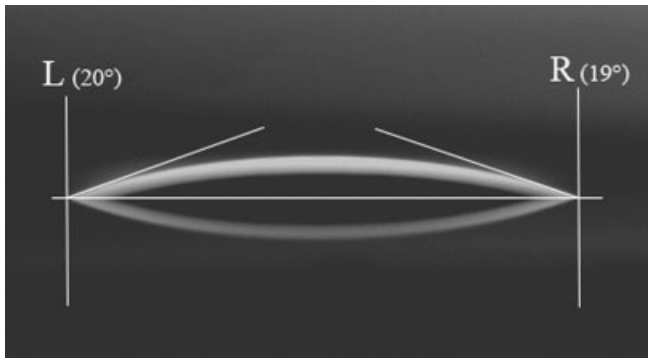

Figure 2. Contact angle image of mussel adhesive protein solution containing 80% Mefp-1 and 20% Mefp-2.

was performed on porcine full thickness skin (North Carolina State University College of Veterinary Medicine, Raleigh, NC), which was inkjetted with adhesive over 1 cm^2 area. Loading rates of 0.6 mm/s and sampling rates of 20 s^{-1} were utilized in this study. The tests were carried out six times for each sample, and a statistical analysis was performed using Student's *t*-test.

RESULTS AND DISCUSSION

The piezoelectric print head utilizes a voltage waveform input that allows control over volume of solution that is dispensed. The waveform varies as a function of viscosity, surface tension and temperature of the jetted solution. The print head moves the ink solution from the cartridge to the channel. The impedance matching unit allows the solution to move through the descender, where it is ejected through a nozzle. In this study, the mussel adhesive protein solution was processed using piezoelectric inkjetting and dropcasting. Images of the drop dispensed at various voltages (Figure 1) were used to estimate the velocity and volume dispensed. For the mussel adhesive protein solution, an increase in firing voltage resulted in a linear increase in jetting velocity. Contact angle measurements (Figure 2) performed on the mussel adhesive protein solutions that were patterned on Si(111) substrates revealed hydrophilic (contact angle <45°) behavior (Table I). No significant difference in contact angle values ($p < 0.05$) for 1:1 Fe:DOPA, 10:1 Fe:DOPA, and 100:1 Fe:DOPA was observed.

TABLE I. Contact Angle Measurements for Mussel Adhesive Protein Solutions (With Varying Iron Concentration) Examined on Si (111) Substrates

Solution on Si (111) Substrate	Contact Angle[a]
Mefp (0.16 m*M* DOPA)	20° ± 2.2°
1:1 Fe:DOPA	18.6° ± 2°
10:1 Fe:DOPA	21.3° ± 1.6°
100:1 Fe:DOPA	22.2° ± 1.9°
Deionized water (Control)	13.2° ± 1.6°

[a] Values are expressed as mean ± SD.

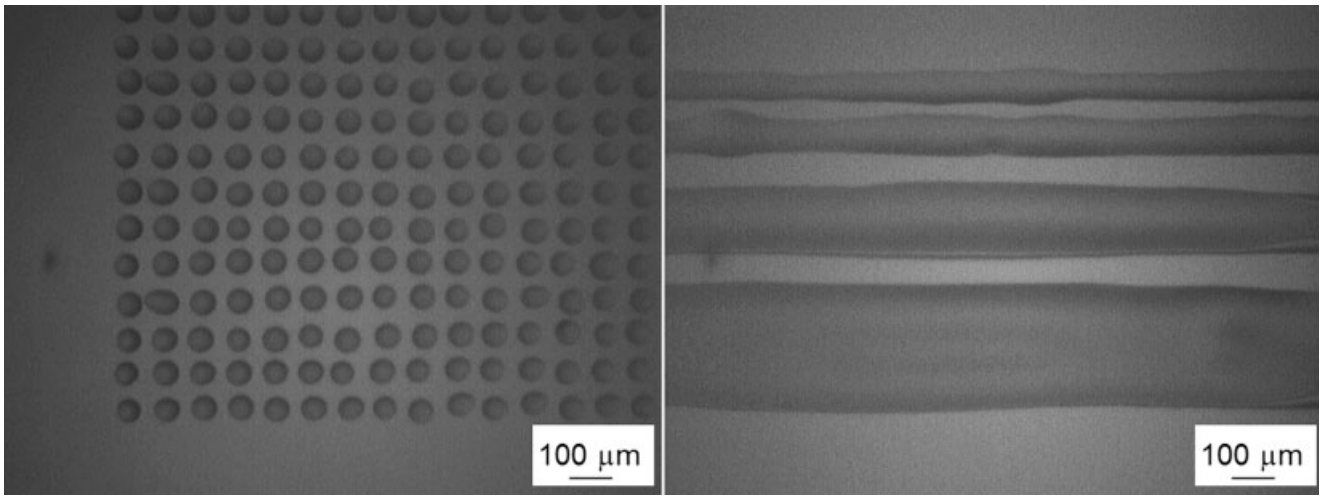

Figure 3. Optical micrographs of mussel adhesive protein solution inkjetted into microarray and line patterns. Scale bar equals 100 μm.

Mussel adhesive protein solutions, $FeCl_3$ solutions, and cyanoacrylate adhesives were successfully deposited in CAD patterns using the piezoelectric inkjet printing system. Inkjetting of mussel adhesive protein solution in microscale patterns with minimum feature size of 50 μm was achieved (Figure 3). Line patterns with widths of ~60, ~90, ~180, and ~300 μm were also fabricated. The typical mammalian cell size is ~10–30 μm. The bonding line-widths of ~60 μm as shown here may be sufficient for microsurgical and other delicate wound closure procedures.

FTIR absorption spectra of inkjetted (at voltages 10, 20, 30, and 40 V) and dropcast mussel adhesive protein materials exhibited similar peak intensity values [Figure 4(A)]. A list of distinct bands for marine mussel adhesive protein materials and their corresponding assignments was previously published by the authors.[17] Amide vibration was observed at ~3250, 1650, 1460, and 1100 cm^{-1} (rocking vibration).[29] C=C stretching was observed at ~1630 cm,[1] and catechol ring vibration was observed between 1300 and 1100 cm^{-1}.[29] O—H stretching vibration was observed between 3600 and 3300 cm^{-1}. The region from 0 to 1000

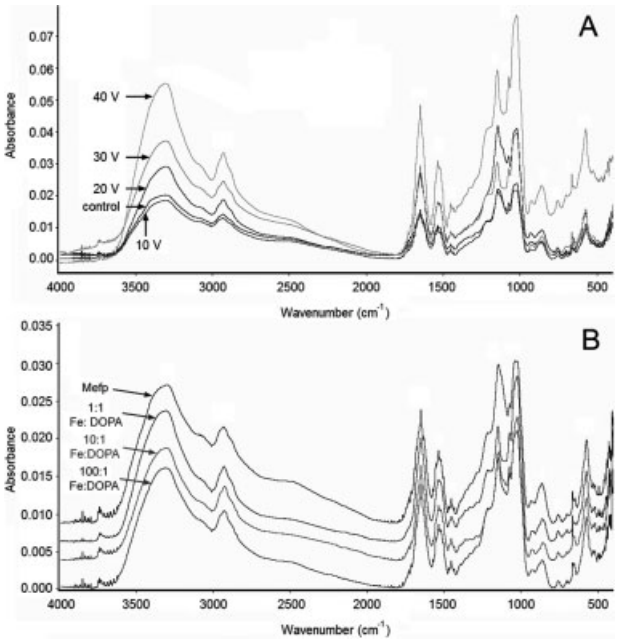

Figure 4. (A) Fourier transform infrared (FTIR) spectra of inkjetted mussel adhesive protein solution (Mefp) as a function of jetting voltage (10–40 V). Control is a dropcast mussel adhesive protein solution. (B) Fourier transform infrared spectra of inkjetted mussel adhesive protein solution (Mefp) as a function of Fe(III) concentration.

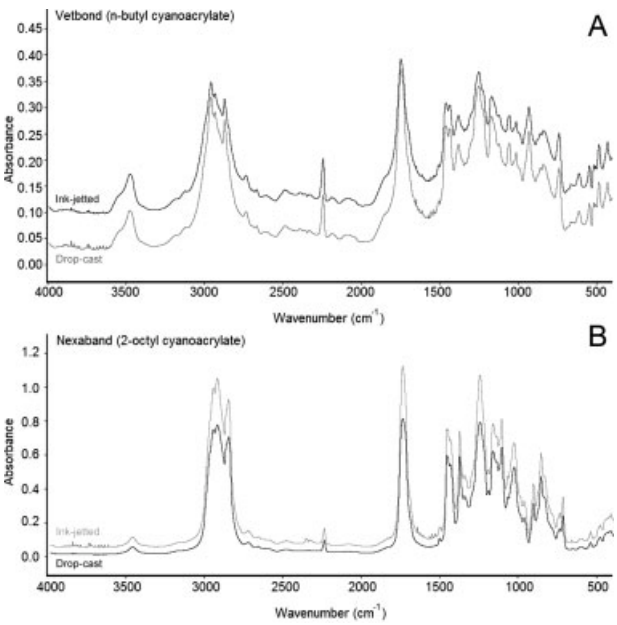

Figure 5. (A) Fourier transform infrared (FTIR) spectra of inkjetted and dropcast n-butyl cyanoacrylate (Vetbond®) materials. Relevant structural peaks are labeled. (B) Fourier transform infrared (FTIR) spectra of inkjetted and dropcast 2-octyl cyanoacrylate (Nexaband®) materials. Relevant structural peaks are labeled.

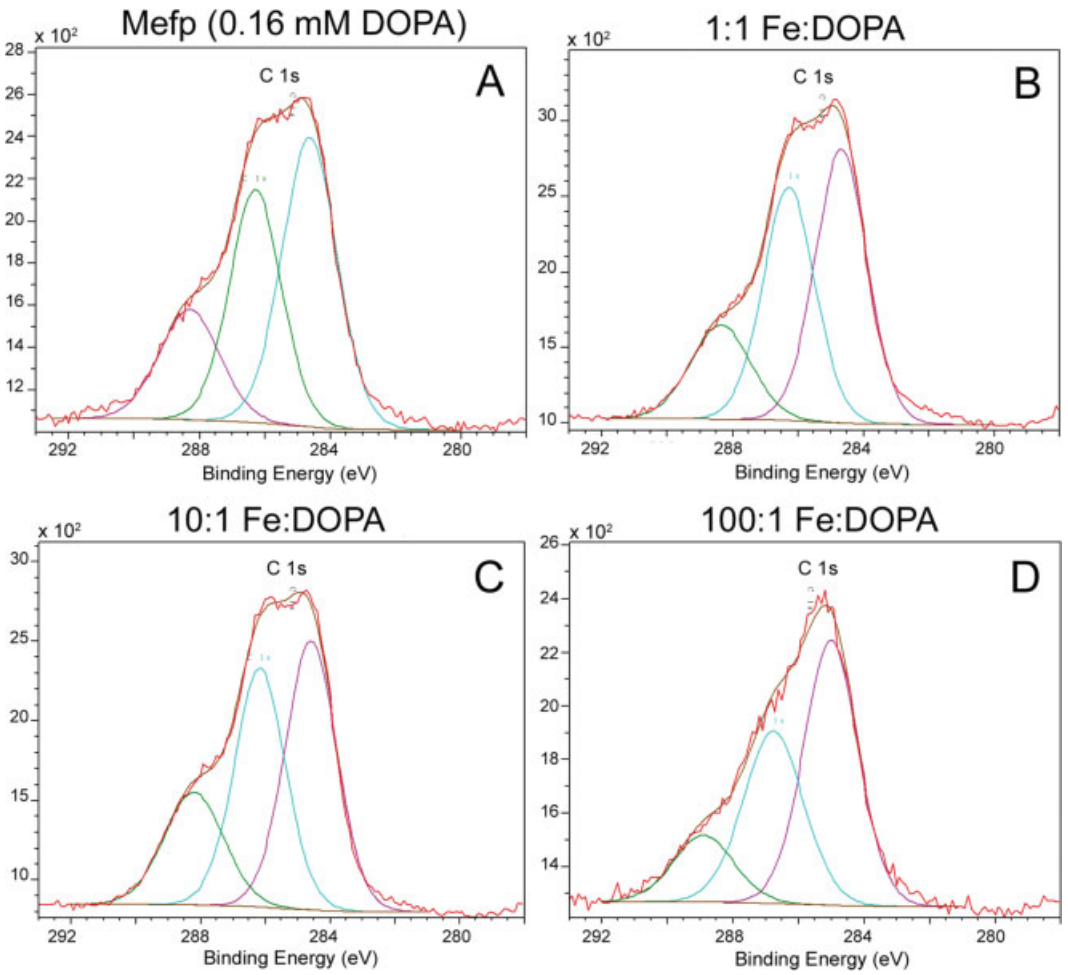

Figure 6. C 1s spectra of inkjetted mussel adhesive protein solutions cured with Fe(III). X-ray photoelectron spectra shown for (A) Mefp (0.16 mM DOPA), (B) 1:1 Fe:DOPA, (C) 10:1 Fe:DOPA, and (D) 100:1 Fe: DOPA. [Color figure can be viewed in the online issue, which is available at www.interscience.wiley.com.]

cm^{-1} contains low-frequency skeletal vibrations, out-of-plane ring deformation, wagging modes of hydrogen atoms, wagging modes of hydroxyl groups on the catechol ring, and wagging modes of carboxylate groups.[29] Significant differences in the absorption peak intensities were observed in materials that were inkjetted at 10, 20, 30, and 40 V. This result may be attributed to the increase in jetting volume that results from an increase in jetting voltage. Similarly, FTIR spectra of inkjetted and dropcast (control) *n*-butyl cyanoacrylate [Figure 5(A)] and 2-octyl cyanoacrylate [Figure 5(B)] revealed similar peak intensity values. FTIR spectra of inkjetted mussel adhesive protein solutions containing iron (in Fe:DOPA ratios of 1:1, 10:1, and 100:1) and as-prepared mussel adhesive protein solution are shown in Figure 4(B). No significant differences in peak intensity values among these materials were observed. The FTIR spectroscopy data suggest that piezoelectric inkjet printing does not significantly alter the structure of the marine mussel adhesive protein or cyanoacrylate adhesives.

X-ray photoelectron spectra of mussel adhesive protein solutions (Figure 6) revealed C—C bonding (corresponding to 285 eV), C—N bonding (corresponding to 286.1 eV), and N—C=O bonding (corresponding to 288.2 eV). The peaks may be attributed to aliphatic and aromatic carbons in the marine mussel adhesive protein material. Deconvolution of the C 1s peak revealed the concentration of various

TABLE II. C 1s Peak Deconvolution from X-Ray Photoelectron Spectra

Assignment	C—C[a]	C—N[b]	N—C=O[c]
Mefp (0.16 M*m* DOPA)	46%	35%	19%
1:1 Fe:DOPA	44	38	18
10:1 Fe:DOPA	42	37	21
100:1 Fe:DOPA	50	36	14

[a] C—C peak corresponds to 285 eV.
[b] C—N peak corresponds to 286.1 eV.
[c] N—C=O peak corresponds to 288.2 eV.

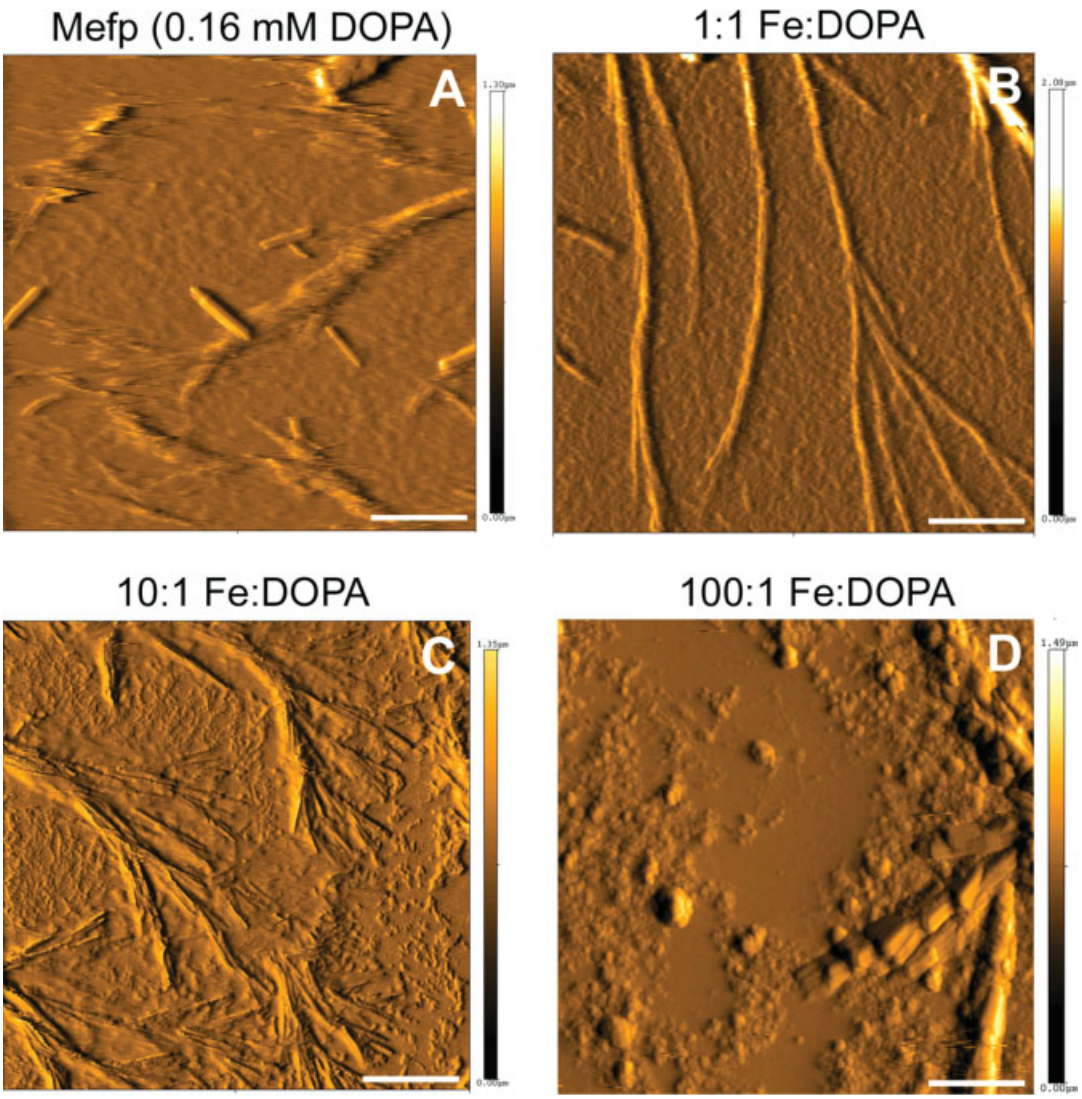

Figure 7. Topography-flattened atomic force micrograph of inkjetted mussel adhesive protein, 1:1 Fe:DOPA, 10:1 Fe:DOPA, and 100:1 Fe:DOPA structures. Scale bar equals 10 μm.

functional groups in inkjetted Fe:DOPA materials (Table II). 1:1 Fe:DOPA and 10:1 Fe:DOPA materials exhibited less C—C bonding than as-prepared Mefp (0.16 mM DOPA) solution. On the other hand, the 100:1 Fe:DOPA material revealed more C—C bonding and less N—C=O bonding than as-prepared Mefp (0.16 m*M* DOPA) solution. X-ray photoelectron spectra of the inkjetted protein solutions were inconclusive in determining the role of Fe(III) in complex formation. However, the distribution of X-ray photoelectron peaks in the inkjet printed materials was similar to that previously observed in spectra of dropcast mussel adhesive proteins (Mefp) materials.[30]

Atomic force microscopy has previously been used to examine the morphology of DOPA-containing residues.[31] An atomic force microscopy of inkjetted mussel adhesive protein solution (Figure 7) revealed cross-linking upon addition of Fe(III). In the absence of iron, mussel adhesive protein (Mefp) [Figure 7(A)] revealed cross-linking and the presence of some fibrous networks. Precipitation of more complex fiber networks was observed in 1:1 Fe:DOPA and 10:1 Fe:DOPA materials [Figure 7(B,C)]. A higher degree

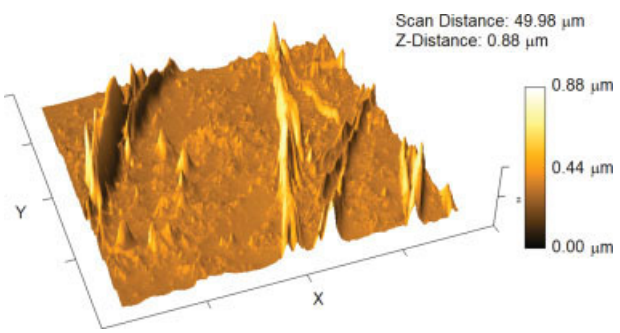

Figure 8. Three-dimensional representation of the surface of mussel adhesive protein solution containing Fe(III) (1:1 Fe:DOPA) obtained using atomic force microscopy. Image was obtained twenty-four hours after curing. [Color figure can be viewed in the online issue, which is available at www.interscience.wiley.com.]

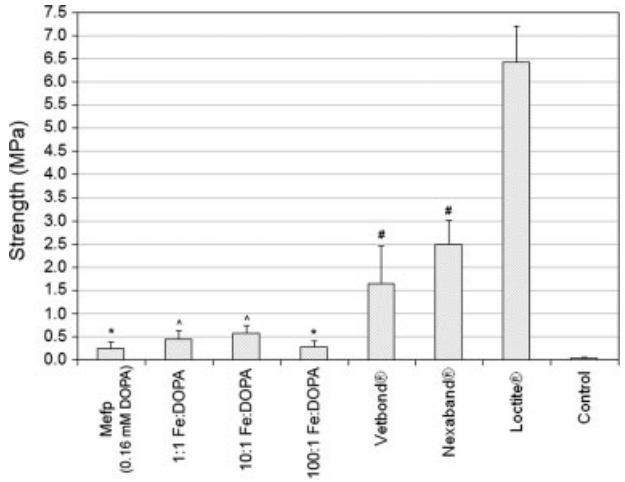

Figure 9. Average strength of bioadhesives inkjetted on full thickness porcine skin. All samples were cured for 24 h. The difference in strength was statistically significant for all except those indicated by "*", "^", and "#" ($p < 0.05$). Bars indicate standard deviation of mean strength.

of cross-linking was observed in the 10:1 Fe:DOPA material than in the 1:1 Fe:DOPA material. Three-dimensional imaging of the surface of the 1:1 Fe:DOPA material revealed high-aspect ratio fibrous network structures (Figure 8). The height of the fibrous networks varied from ~400 to ~800 nm, while the width of fibrous networks varied from ~500 to ~5 μm. The 100:1 Fe:DOPA material revealed islands of cross-linked mussel adhesive protein material (Figure 7D). Small regions of fibrous networks were observed within the inkjetted pattern, which result from nonuniform distribution of mussel adhesive protein in the inkjetted solution. Previous studies have demonstrated iron-induced cross-linking of mussel adhesive proteins using electron paramagnetic, infrared, and ultraviolet-visible absorption spectroscopies.[22,33]

Adhesion characteristics of pure marine mussel extracts have been previously examined under different curing conditions (Figure 9).[34,35] Low humidity and nonoxidative conditions have been shown to be critical in obtaining strong adhesion properties in mussel adhesive proteins. Tensile testing of inkjetted materials on full-thickness porcine skin revealed that mussel adhesive proteins exhibit significantly lower adhesion strength values than cyanoacrylate adhesives (Figure 9). Inkjetted ethyl cyanoacrylate (Quick Set™ Loctite®) showed highest strength among tested adhesives. Inkjetted *n*-butyl cyanoacrylate (Vetbond®) and 2-octyl cyanoacrylate (Nexaband®) patterns exhibited similar adhesion strength values; however, the toxic effects of these materials are well-documented.[6–8] Addition of Fe(III) to Mefp (0.16 m*M* DOPA) in 1:1 Fe:DOPA improved adhesion strength. The 10:1 Fe:DOPA and 1:1 Fe:DOPA materials did not exhibit significant differences in adhesion strength. However, the 100:1 Fe:DOPA material exhibited lower adhesion strength values than the 1:1 Fe:DOPA and 10:1 Fe:DOPA materials. This finding suggests that the relatively low adhesion strength of the 100:1 Fe:DOPA material results from a high degree of cross-linking within the mussel adhesive protein material, which limits interaction with the porcine skin substrate. In addition, two different ferric catecholate complexes may be formed at low and high Fe:DOPA ratios.[21] Previous studies have shown that iron (III) can serve as a cross-linking agent for mussel adhesive protein.[36–38] For example, previous electron paramagnetic resonance studies have confirmed iron-induced cross-linking in precursor proteins, which is similar to that observed in intact mussel plaques.[22] The atomic force microscopy images for the 1:1 and 10:1 Fe:DOPA materials contain a relatively high density of fibrous networks. On the other hand, a relatively low density of fibrous networks is observed in the Mefp (0.16 m*M* DOPA) and 100:1 Fe:DOPA materials. The density of fibrous networks may be correlated with the adhesion strength observed in mussel adhesive protein materials. These results suggest that the extent of cross-linking and precipitation in these inkjetted mussel adhesive protein patterns may be correlated with iron concentration. As discussed earlier, metal-mediated catechol complexation is thought to be responsible for the adhesion properties of mussel adhesive proteins.

CONCLUSIONS

Mussel adhesive proteins could serve as environmentally friendly alternatives to synthetic adhesives in biomedical, electronics, and marine-equipment applications. Fourier transform infrared spectra and X-ray photoelectron spectra have shown that piezoelectric inkjetting is a nondestructive technique that may be successfully used to dispense picoliter amounts of mussel adhesive proteins and other adhesives. Atomic force microscopy and adhesion testing have demonstrated that the adhesive strength in these materials may be correlated with the amount of iron-induced cross-linking. CAD ink-jetting of naturally-derived mussel adhesive proteins such as *Mytilus edulis* foot proteins may overcome several problems associated with conventional medical adhesives. This technology may greatly improve wound repair in next generation eye repair, fracture fixation, wound closure, and drug delivery devices.

REFERENCES

1. Ginsberg SP, Polack FM. Cyanoacrylate tissue adhesive in ocular disease. Ophthalmic Surg 1972;3:126–132.
2. Landegren T, Risling M, Persson JKE. Local tissue reactions after nerve repair with ethyl-cyanoacrylate compared with epineural sutures. Scand J Plast Reconstr 2007;41:217–227.
3. Eskandari MM, Ozturk OG, Eskandari HG, Balli E, Yilmaz C. Cyanoacrylate adhesive provides efficient local drug delivery. Clin Orthop Relat Res 2006;451:242–250.
4. Applebaum JS, Zalut T, Applebaum D. The use of tissue adhesion for traumatic laceration repair in the emergency department. Ann Emerg Med 1993;22:1190–1192.

5. Vanholder R, Misotten A, Roels H, Matton G. Cyanoacrylate tissue adhesive for closing skin wounds- a double-blind randomized comparison with sutures. Biomaterials 1993;14:737–742.
6. Hauptmann M, Lubin JH, Stewart PA, Hayes RB, Blair A. Mortality from lymphohematopoietic malignancies among workers in formaldehyde industries. J Nat Cancer Inst 2003;95:1615–1623.
7. Pinkerton LE, Hein MJ, Stayner LT. Mortality among a cohort of garment workers exposed to formaldehyde: an update. Occup Environ Med 2004;61:193–200.
8. Leggat PA, Smith DR, Kedjarune U. Surgical applications of cyanoacrylate adhesives: A review of toxicity. Aust NZ J Surg 2007;77:209–213.
9. Dunn CJ, Goa KL. Fibrin sealant—A review of its use in surgery and endoscopy. Drugs 1999;58:863–886.
10. Sierra DH. Fibrin sealant adhesive systems: A review of their chemistry, material properties, and clinical applications. J Biomater Appl 1993;7:309–352.
11. Clark RA. Fibrin glue for wound repair: Facts and fancy. Thromb Haemost 2003;90:1003–1006.
12. Schreiber GB, Busch MP, Kleinman SH, Korelitz JJ. The risk of transfusion-transmitted viral infections. New Engl J Med 1996;334:1685–1690.
13. Lin Q, Gourdon D, Sun C, Holten-Andersen N, Anderson TH, Waite JH, Israelachvili JN. Adhesion mechanisms of the mussel foot proteins mfp-1 and mfp-3. Proc Natl Acad Sci USA 2008;104:3782–3786.
14. Waite JH, Housley TJ, Tanzer ML. Peptide repeats in a mussel glue protein- theme and variattions. Biochemistry 1985;24:5010–5014.
15. Waite JH. Natures underwater adhesive specialist. Int J Adhes Adhes 1987;7:9–14.
16. Olivieri MP, Baier RE, Loomis RE. Surface properties of mussel adhesive protein-component films. Biomaterials 1992;13: 1000–1008.
17. Doraiswamy A, Narayan RJ, Cristescu R, Mihailescu IN, Chrisey DB. Laser processing of natural mussel adhesive protein thin films. Mater Sci Eng C. 2007;27:409–413.
18. Waite JH. Adhesion a la Moule. Integr Comp Biol 2002;42:1172–1180.
19. Wiegemann M. Adhesion in blue mussels (Mytilus edulis) and barnacles (genus Balanus): Mechanisms and technical applications. Aquat Sci 2005;67:166–176.
20. Taylor SW, Chase DB, Emptage MH, Nelson MJ, Waite JH. Ferric ion complexes of a DOPA-containing adhesive protein from Mytilus edulis. Inorg Chem 1996;35:7572–7577.
21. Monahan J, Wilker JJ. Specificity of metal ion cross-linking in marine mussel adhesives. Chem Commun 2003;14:1672–1673.
22. Sever MJ, Weisser JT, Monahan J, Srinivasan S, Wilker JJ. Metal-mediated cross-linking in the generation of a marine-mussel adhesive. Angew Chem Int Ed 2004;43:448–450.
23. Waite JH, Andersen NH, Jewhurst S, Sun CJ. Mussel adhesion: Finding the tricks worth mimicking. J Adhes 2005;81: 297–314.
24. Lemmo AV, Rose DJ, Tisone TC. Inkjet dispensing technology: applications in drug discovery. Curr Opin Biotechnol 1998;9:615–617.
25. Calvert P. Inkjet printing for materials and devices. Chem Mater 2001;13:3299–3305.
26. Roth EA, Xu T, Das M, Gregory C, Hickman JJ, Boland T. Inkjet printing for high-throughput cell patterning. Biomaterials 2004;25:3707–3715.
27. Sumerel J, Lewis J, Doraiswamy A, Deravi LF, Sewell SL, Gerdon AE, Wright DW, Narayan RJ. Piezoelectric ink jet processing of materials for medical and biological applications. Biotechnol J 2006;1:976–987.
28. Waite JH. Precursors of quinone tanning-dopa-containing proteins. Method Enzymol 1995;258:1–20.
29. Weinhold M, Soubatch S, Temirov R, Rohlfing M, Jastorff B, Tautz FS, Doose C. Structure and bonding of the multifunctional amino acid L-DOPA on Au(110). J Phys Chem B 2006;110:23756–23769.
30. Baty AM, Suci PA, Tyler BJ, Geesey GG. Investigation of mussel adhesive protein adsorption on polystyrene and poly(octadecyl methacrylate) using angle dependent XPS. ATR-FTIR, and AFM. J Colloid Interface Sci 1996;177:307–315.
31. Lee H, Scherer NF, Messersmith PB. Single-molecule mechanics of mussel adhesion. Proc Natl Acad Sci USA 2006;103:12999–13003.
32. Weisser JT, Nilges MJ, Sever MJ, Wilker JJ. EPR investigation and spectral simulations of iron-catecholate complexes and iron-peptide models of marine adhesive cross-links. Inorg Chem 2006;45:7736–7747.
33. Sever MJ, Wilker JJ. Absorption spectroscopy and binding constants for first row transition metal complexes of a DOPA-containing peptide. Dalton Trans 2006;6:813–822.
34. Ninan L, Monahan J, Stroshine RL, Wilker JJ, Shi RY. Adhesive strength of marine mussel extracts on porcine skin. Biomaterials 2003;24:4091–4099.
35. Schnurrer J, Lehr CM. Mucoadhesive properties of the mussel adhesive protein. Int J Pharm 1996;141:251–256.
36. Monahan J, Wilker JJ. Reagents for cross-linking the protein precursor of a marine mussel adhesive. Langmuir 2004;20: 3724–3729.
37. Loizou E, Weisser JT, Schmidt G, Wilker JJ. Effects of iron ion cross-linking on biopolymer hydrogels. Macromol Biosci 2006;6:711–718.
38. Hight LM, Wilker JJ. Synergestic effects of metals and oxidation in the curing of marine mussel adhesive. J Mater Sci 2007;42:8934–8942.